

CHAPTER 8

NON-SCINTILLATOR APPLICATIONS OF PHOTOMULTIPLIERS

8.1 Analytical applications

- 8.1.1 Bioluminescence
- 8.1.2 Chemiluminescence
- 8.1.3 Flame spectrometry
- 8.1.4 Raman spectrometry

8.2 Non-analytical applications

- 8.2.1 Image conversion
- 8.2.2 Laser scanners
- 8.2.3 Laser telemetry

8.3 Cherenkov radiation

8.4 Cherenkov experiments

- 8.4.1 High-energy physics experiments
- 8.4.2 Proton decay experiments
- 8.4.3 Solar neutrino experiments
- 8.4.4 Neutrino oscillation experiments
- 8.4.5 DUMAND experiments
- 8.4.6 Air-shower experiments
- 8.4.7 Towards a common goal
- 8.4.8 A vital tool for physics

NON-SCINTILLATOR APPLICATIONS OF PHOTOMULTIPLIERS

Scintillation counting is by no means the only application of photomultipliers. Many applications exist in which the photomultiplier tube itself is used as a low light-level detector. The brief survey given here is meant only to convey an impression of the diversity of applications in which, because of their large-area sensitivity, gain, and time characteristics, photomultipliers continue to be the detectors of choice – or are but slowly yielding to new solid-state rivals.

8.1 Analytical applications

8.1.1 *Bioluminescence*

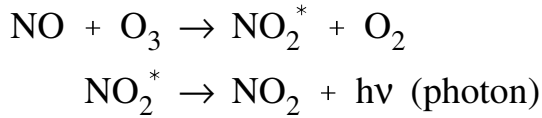
The availability of suitable reagents has stimulated interest in bioluminescence as an analytical technique. Bioluminescence assay of adenosine triphosphate (ATP), for example, is possible using the luciferin-luciferase ('firefly') reaction.

Because of the extremely low light levels produced in such reactions, single photon counting is required and signals have to be integrated over intervals of some seconds; the reaction can be followed by comparing the luminous activity during successive intervals. Tolerable noise levels are so low that photomultipliers often have to be specially selected to satisfy specifications calling for less than a few hundred counts per second above a threshold corresponding to a fraction of a photoelectron. Moreover, since the spectrum of bioluminescence is between 460 nm and 580 nm, maximum green sensitivity combined with low noise is required. Since these are conflicting requirements, a fine balance has to be found between them in the preparation of the bialkali cathodes to assure optimum performance. Finally, to provide sufficient gain, tubes with 11 or 12 stages are needed.

8.1.2 *Chemiluminescence*

Although the light produced by a chemiluminescent reaction is characteristic of the reaction, the spectrum is wide (Fig.8.1) and not easy to analyse to identify the reacting substances. Analysis is therefore based on prior choice of a reagent known to chemiluminescence with the substance sought and optical filtering to limit the detector response to an analytically significant part of the spectrum.

Chemiluminescence has been widely used for qualitative and quantitative analysis of air pollution. The concentration of ozone, for example, can be measured by its reaction with ethylene or with rhodamine B; the latter gives high luminous efficiency but depends on the surface state of the rhodamine. Nitric oxide can be measured by its reaction with ozone,



As with the NO_2^* , molecules can also lose their excitation energy by collision with other molecules, without radiation; the reaction is carried out at a pressure of only a few hundred pascals (Fig.8.2). The intensity of the luminescence is proportional to the concentration of NO; using photomultipliers it is possible to measure concentrations as small as a few parts per billion (ppb = 10^{-9}). In air pollution assays, the total concentration of NO plus NO_2 can be measured by first reducing the NO_2 to NO.

As the reaction chamber excludes background light, it is possible to reduce noise and increase sensitivity by synchronous detection (§5.13.2); however, it is more usual merely to minimize dark count by cooling the photocathode.

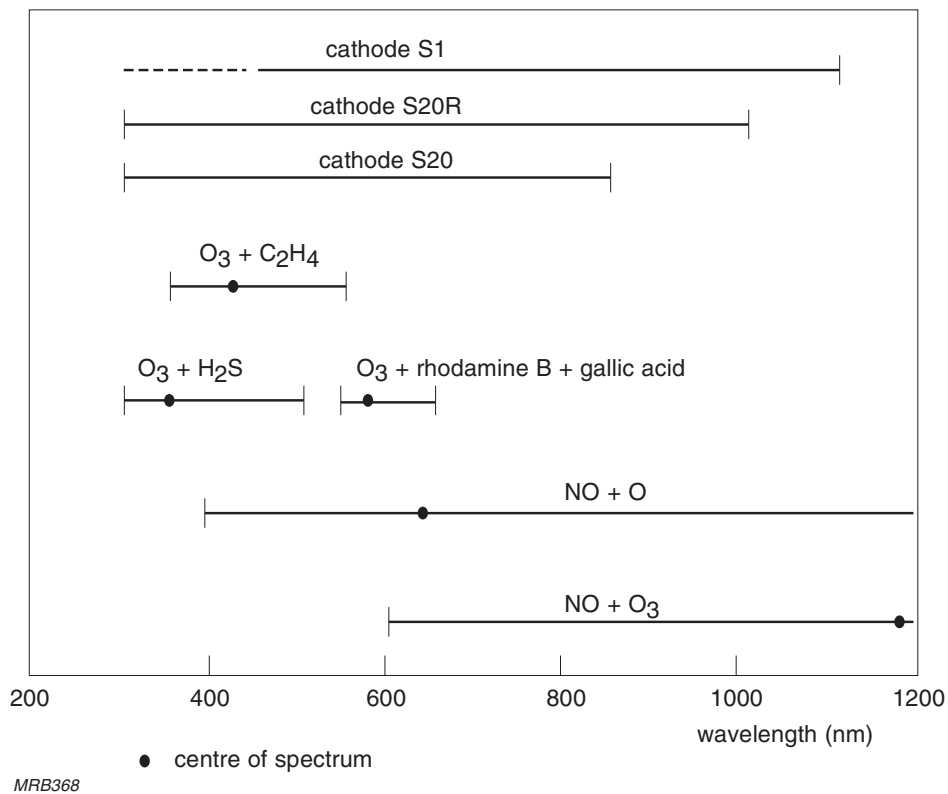


Fig.8.1 Spectra over which various chemiluminescent substances radiate compared with the spectra over which S1, S20 and S20R photocathodes respond

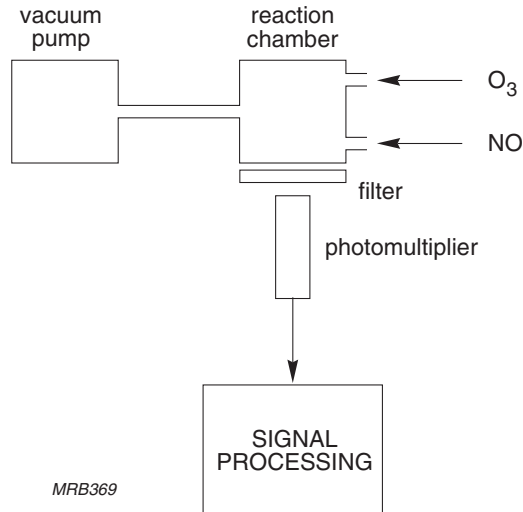


Fig.8.2 Measurement of chemiluminescence

Recently, chemiluminescence light immuno-assay (CLIA or LIA) has become a strong competitor of RIA (§7.2.2) as a sensitive analytical tool. Instead of using ^{125}I isotopes (as in RIA), CLIA uses acridinium esters which emit photons at around 430 nm when they oxidize. This wavelength is ideal for detection by standard SbKCs low-noise photomultipliers.

8.1.3 Flame spectrometry

Flame spectrometry can be based on either emission (bright-line) or absorption (dark-line) spectra. Emission is commonly used for identifying the constituent elements of a specimen and measuring their concentrations; absorption, for measuring the concentrations of elements already known, or suspected, to be present in a specimen.

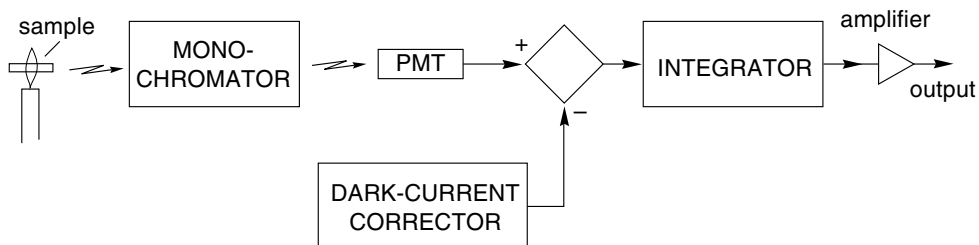


Fig.8.3 Principle of emission spectrometry

Figure 8.3 shows an emission spectrometer in which a monochromator isolates spectral lines corresponding to the constituent elements of the specimen and a photomultiplier measures the line intensities to determine the element concentrations. The spectrum due to the flame alone can be excluded by moving the specimen into and out of the flame for equal intervals and synchronously switching the gain between +1 and -1 (Fig.8.4); this also cancels the effect of the photomultiplier dark current.

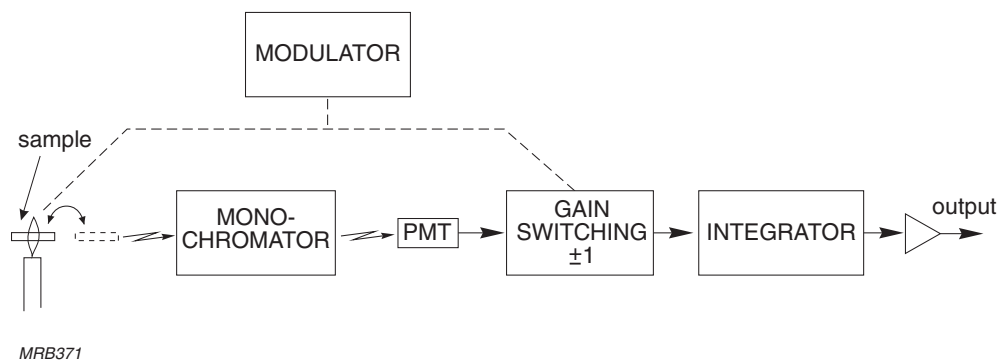
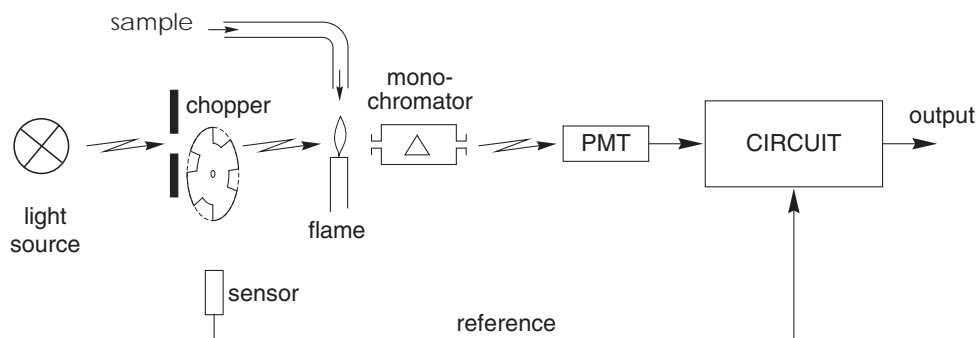


Fig.8.4 Measures for excluding dark current effects and the spectrum of the flame

Figure 8.5 shows an absorption spectrometer as used for measuring small concentrations, mainly of metallic elements, in aqueous or organic solutions (see Table 8.1). The vaporized specimen, reduced partly to the atomic state by the flame, is traversed by effectively monochromatic light of a wavelength chosen to reveal absorption by the element sought; hollow-cathode gas-discharge lamps are commonly used as light sources. By measuring the amount of absorption at each wavelength investigated, the photomultiplier determines the concentration of the corresponding elements. Reference solutions of known composition and concentration are used to calibrate the instrument.

As in the emission spectrometer, the spectrum of the flame itself is a disturbing factor. Its influence can be cancelled either by chopping the light from the monochromatic source and using synchronous detection, as in the arrangement shown, or by comparing measurements made with and without the specimen.



MRB378

Fig.8.5 Principle of absorption spectrometry

Table 8.1 Absorption spectrometry excitation wavelengths and detection thresholds of some elements in aqueous solution

element	wavelength (nm)	detection threshold ($\mu\text{g/ml}$)	element	wavelength (nm)	detection threshold ($\mu\text{g/ml}$)
Ag	328.1	0.002	Mo	313.3	0.04
Al	309.3	0.02	Na	589.0	0.0005
As	193.7	0.1	Nb	334.9	4
Au	242.8	0.03	Ni	232.0	0.01
B	249.8	3.0	Pb	217.0	0.02
Ba	553.6	0.03	Pd	244.8	0.03
Be	234.9	0.002	Rb	780.0	0.001
Bi	223.1	0.04	Sb	217.6	0.05
Ca	422.7	0.002	Se	196.0	0.3
Cd	228.8	0.002	Si	251.6	0.2
Co	240.7	0.01	Sn	224.6	0.05
Cr	357.9	0.005	Sr	460.7	0.006
Cs	852.1	0.01	Ta	271.5	4
Cu	324.8	0.003	Te	214.3	0.5
Fe	248.3	0.018	Ti	364.3	0.1
Hg	253.7	0.2	Tl	276.8	0.03
In	303.9	0.05	V	318.5	0.05
K	766.5	0.003	W	255.1	2
Li	670.8	0.002	Y	410.2	0.3
Mg	285.2	0.0002	Zn	213.9	0.001
Mn	279.5	0.003			

8.1.4 Raman spectrometry

Raman spectrometry is based on wavelength shifts due to inelastic scattering of photons when light passes through a transparent medium; it is a molecular phenomenon with no atomic counterpart. The observed shifts are characteristic of the molecular structure of the medium.

Because of the very low relative intensity of the scattered light, Raman spectrometry is practical only with a high-intensity light source for excitation. The appearance of industrial lasers has in recent years led to its widespread adoption as a means of measuring air pollution (Fig.8.6); Table 8.2 lists some of the lasers used, and Table 8.3 the Raman-effect wavelength shifts observable for several atmospheric gases excited by a nitrogen laser.

The amount of wavelength shift due to the Raman effect depends solely on the molecular structure of the medium and not on the wavelength of the excitation light. However, as the intensity of the light at the shifted wavelength varies inversely as the fourth power of the excitation wavelength, it is best to choose the shortest wavelength consistent with the spectral response of the detector used. To obtain a sufficiently high signal-to-noise ratio, the detector chosen is usually a high-gain photomultiplier which, for maximum sensitivity, may be operated as a photon counter (§5.13.3).

Table 8.2 Wavelengths and mean output powers of lasers used in Raman spectrometry

laser	λ (nm)	P_o mean (mW)
helium-cadmium	325	15
helium-cadmium	441.6	50
nitrogen	337.1	
ruby with frequency doubler	347.1	
argon	488	50 – 2000
argon	514.5	50 – 2000
neodymium ((YAG) with frequency doubler	530	
krypton	530.8	100 – 400
krypton	568.2	100 – 400
krypton	647.1	100 – 400
helium-neon	632.8	10 – 200
ruby (quasi continuous)	694.3	1000

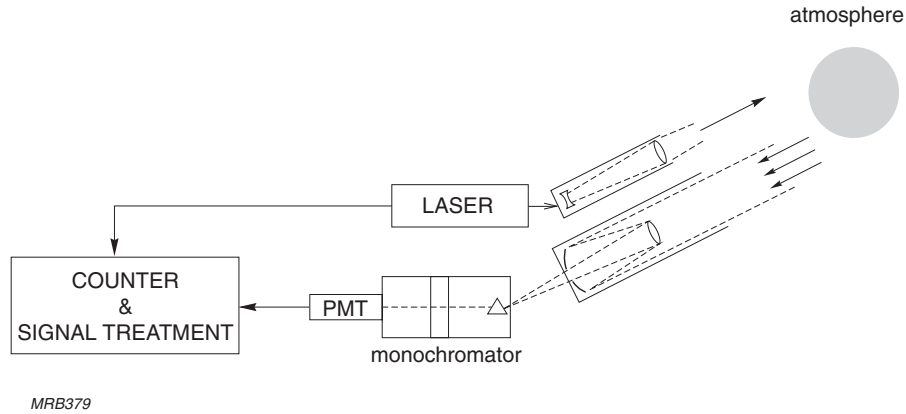


Fig.8.6 Principle of Raman spectrometry for measuring atmospheric pollution using a laser as the excitation light source

Table 8.3 Raman-effect wavelengths λ_r and wave-number shifts $\Delta\sigma$ ($\sigma = 1/\lambda$) in some molecular gases excited at a wavelength of 337.1 nm

	CO ₂ (2v ₂)	CO ₂ (v ₁)	O ₂	CO	N ₂	CH ₄ (v ₁)	CH ₄ (v ₂)	H ₂ O (v ₁)	H ₂	
λ_r	352.4	353.7	355.7	363.4	365.8	373.8	375.3	384.4	392.1	nm
$\Delta\sigma$	1285.5	1388.3	1554.7	2145.0	2330.7	2914.2	3020.3	3651.7	4160.2	cm ⁻¹

8.2 Non-analytical applications

8.2.1 Image conversion

Photomultipliers have been used for many years in the flying-spot scanners that convert photo-transparencies into video signals for television transmission (Fig.8.7). A television raster traced on the screen of a very-short-persistence cathode-ray 'flying-spot' tube is focused on the transparency to be televised. On the other side of the transparency a photomultiplier converts the transmitted light into a signal synchronous with the raster scan. Good uniformity of anode sensitivity is an important requirement, and in a three-tube scanner for colour television each tube must also have high monochromatic cathode sensitivity; in the red channel, tubes with S20 cathodes give the best signal-to-noise ratio. Another requirement is that, for adequate bandwidth (about 5 MHz), the anode load must be small and the tube must be able to operate stably at the high anode currents used. This is therefore one of the few applications where the life of the photomultiplier tube is critical and where it is quite common for the tubes to need replacing every year.

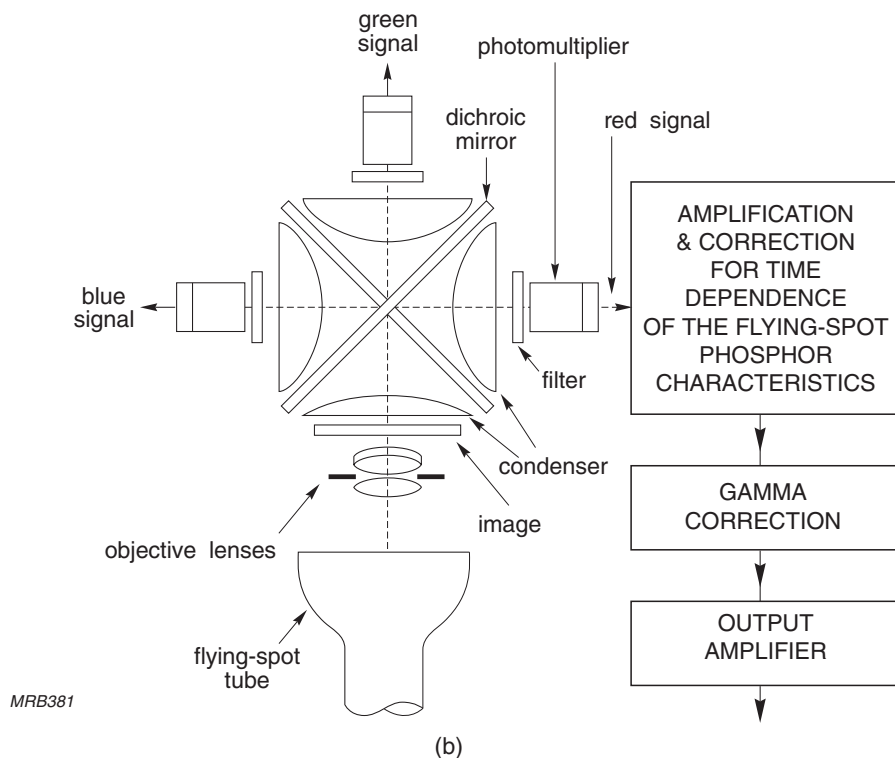
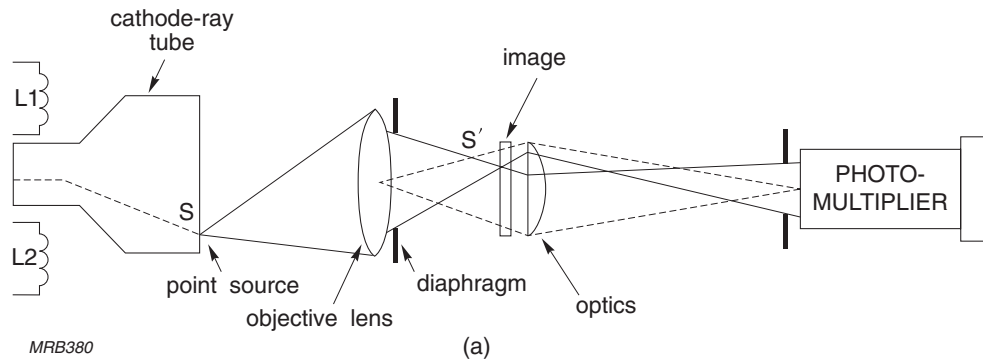


Fig.8.7 Conversion of photo-transparencies into a video image using a flying-spot scanner and photomultiplier tubes (a) monochrome system, (b) three-colour system

8.2.2 Laser scanners

Helium-neon lasers are frequently used in scanners for facsimile machines and bar-code readers, sometimes with photomultipliers as detectors.

In facsimile machines an important requirement is that the photomultiplier gain should show little hysteresis after several milliseconds' exposure to a high light level. As the facsimile scanning system often includes rapidly moving mechanical and

optical parts, high immunity to microphony is also important. These days, linear silicon diode arrays are often used in place of photomultipliers in facsimile scanners.

Large detection area, good time characteristics, and low noise made photomultipliers a natural first choice for use in scanners for reading the Universal Product Code (UPC), the bar identification code nowadays found on many packages. However, in such a scanner a photomultiplier has to draw a continuous anode current of 50 to 80 μA , which causes large gain changes (e.g. 5% to 20%) during the first thousand hours of life and a gradual degradation of gain over the next few thousand hours. Because of this the tubes had to be regularly replaced. Improvements in scanner optics have since made it possible to use large-area silicon photodiodes as detectors. However, in fast drum scanners for reproducing high-quality colour posters or scanning colour photographs for 'catalogue' presentations, the photomultiplier remains the first choice as detector.

In certain industrial scanning applications, such as the detection of surface defects in paper and rolled steel, where optical design is made difficult by the large areas to be scanned, large-diameter, red-sensitive photomultipliers are still preferred.

8.2.3 *Laser telemetry*

Distances to remote objects can be measured by timing the reflection of laser pulses from them. With electronics capable of resolving 5 ns intervals, accuracies within 75 cm can be obtained over ranges limited only by atmospheric absorption or the earth's curvature. With more precise electronics, accuracy is proportionately greater. The estimated 150 cm inaccuracy in the distance from the earth to the moon measured by laser-pulse reflection in 1969 was due largely to the experimental error, which becomes significant over such a distance, in the then accepted value of the velocity of light.

In the telemetry set-up illustrated in Fig.8.8 the transmitted laser pulse opens the timing gate and the reflected pulse closes it. The interference filter limits the photomultiplier response to the same wavelength as the laser pulse. Nevertheless, background light of that wavelength and photomultiplier dark pulses can both give rise to spurious responses. To a large extent these can be excluded by adjustment of the detection threshold. They can be still further reduced by using a coincidence detector as shown in Fig.8.9. If the pulses from both photomultipliers are shaped to a width τ corresponding to that of the laser pulses, the mean frequency of random coincidences is $n = 2n_1n_2\tau$, where n_1 and n_2 are the mean frequencies of the dark pulses from photomultipliers 1 and 2.

The frequency of random coincidences can itself be minimized by setting a range window that brackets the estimated distance to be measured. This not only improves sensitivity but also makes it possible in many cases to use low-power lasers that operate at or near the peak of the photomultiplier sensitivity curve (i.e. below 700 nm).

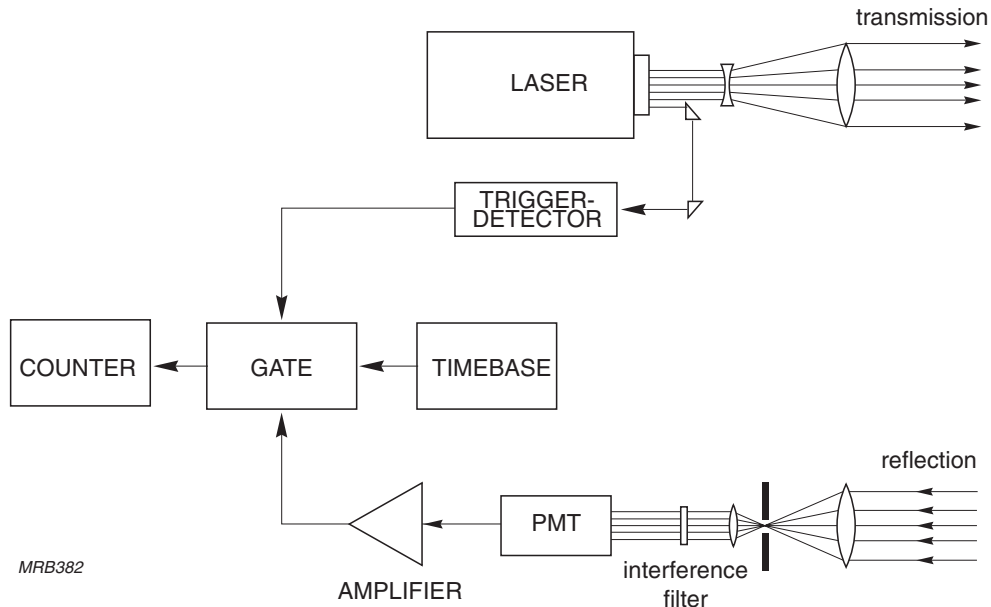


Fig.8.8 Principle of laser telemetry

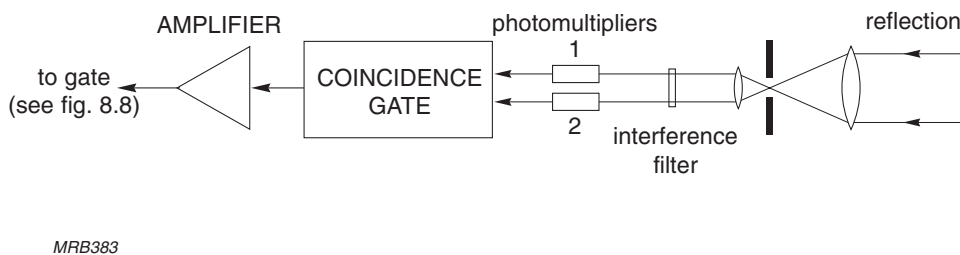


Fig.8.9 The use of a coincidence detector to reduce spurious responses in laser telemetry

Solid state lasers suitable for long-range telemetry can generate 10 ns pulses with a peak power of about a megawatt at a repetition rate of up to 50 per second. Neodymium-doped YAG and glass lasers emit at a wavelength of 1060 nm, ruby lasers at 694 nm. With the aid of frequency-doubling crystals these wavelengths can be halved to 530 nm (green) and 347 nm (near-ultraviolet) respectively, which are closer to the peak sensitivity wavelengths of most photomultipliers.

Semiconductor lasers suitable for short-range telemetry generate similar pulse widths but much lower peak powers (about a watt); their pulse repetition rates can be as high as 1000 per second.

For best resolution, the photomultipliers should be fast-response types. However, if compactness or cost is more important than resolution, as in some industrial applications, small-diameter general-purpose types will do.

An example of laser telemetry is local laser communication between buildings where the photomultiplier's good signal-to-noise ratio, large area and speed makes it the preferred detector over silicon or avalanche photodiodes.

8.3 Cherenkov radiation

Cherenkov radiation is polarized light generated when a charged particle moves through a medium faster than the speed of light in the medium. At an angle to the path of the particle the light is reinforced by constructive interference so that a conical wavefront is formed with the particle at its apex; the phenomenon is an electromagnetic counterpart of the shock wave generated by a supersonic aircraft or the bow wave of a ship. The half-angle of the conical wavefront is $\theta = \arccos(c/nv)$, where c is the speed of light in vacuum, n the refractive index of the medium, and v the speed of the particle. With the aid of photomultipliers it is possible to measure the angle of the wavefront by measuring the radius of the projected 'Cherenkov ring' (Fig.8.10) and thereby to determine the speed of the particle; if the type of particle is known, its energy can also be calculated. By suitable configuration of the optics it is also possible to make the photomultiplier respond only to particles of a specific speed. As the light pulses are practically instantaneous, Cherenkov detectors are often used as triggers in high-energy physics experiments.

The number of detected photoelectrons is given by the so-called Cherenkov radiation formula:

$$n_e = N_0 L \sin^2\theta \quad (8.1)$$

with

$$N_0 = \frac{2\pi}{137} \int_{\lambda_1}^{\lambda_2} \rho(\lambda) t(\lambda) r(\lambda) \frac{d\lambda}{\lambda^2} \quad (8.2)$$

and in which $\rho(\lambda)$ is the quantum efficiency of the counter and $t(\lambda)$ the transparency of the Cherenkov medium and $r(\lambda)$ the reflectivity of the mirrors used. If no mirrors

are used $r = 1$. L is the particle track length in the Cherenkov medium and θ is the angle of the Cherenkov radiation relative to the particle trajectory.

In practice, N_0 is around 50/cm for glass-window tubes and around 100/cm for quartz-window tubes. As $\sin^2\theta$ is small, these values for N_0 mean that gas Cherenkov counters always tend to be rather long. Also, since N_0 increases with the proportion of the UV spectrum that can be used (from Eq.8.2), Cherenkov counters tend to use fast-response quartz-window tubes, often as large as 5 inches in diameter to catch as much of the UV light as possible. Since such tubes are expensive, recent practice has been to use standard tubes optimized for visible light and to shift the UV component into the visible spectrum by covering the tube window with a wavelength shifting layer of, for example TPB (tetraphenyl-butadiene) or PTP (1,4 diphenylbenzol). Disadvantages here, however, are that the layers must be deposited under vacuum and that they are somewhat unstable.

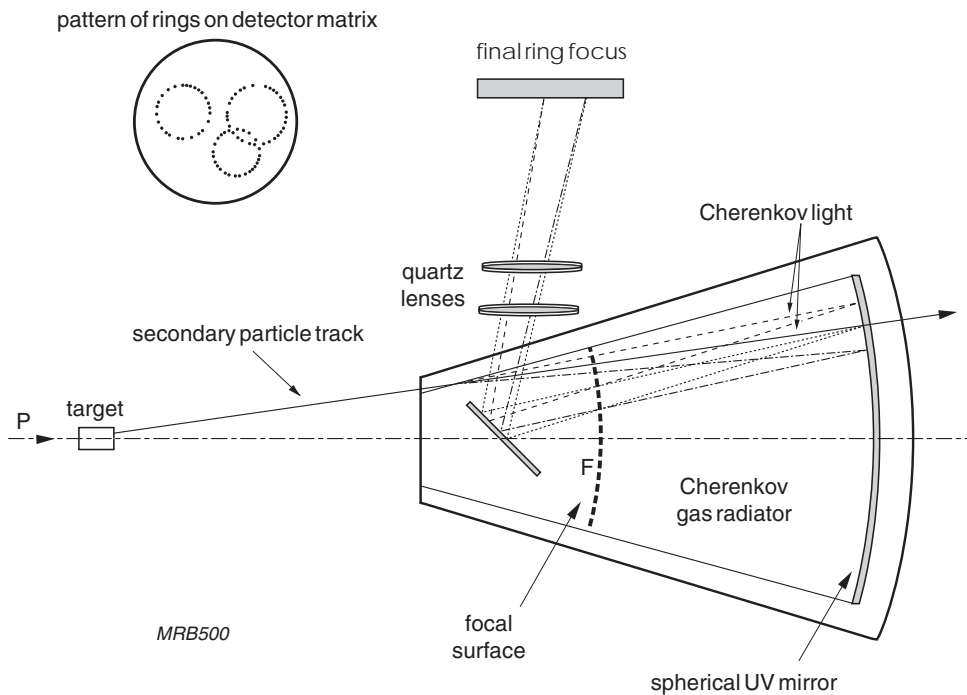


Fig.8.10 Cherenkov detector optical system in ring-focusing mode (courtesy of CERN, Geneva)

8.4 Cherenkov experiments

8.4.1 High-energy physics experiments

In high-energy physics experiments it is often of interest to discriminate particles that exceed a certain minimum speed. This can be done by choosing a Cherenkov medium, often a gas, with an index of refraction corresponding to that minimum speed. Indices as low as 1.03 can be obtained with recently developed solid materials

called *aerogels* which can be shaped into blocks. This has led to the development of large veto-counter boxes where the Cherenkov light produced by electrons, pions or kaons in about 5 cm thick aerogel blocks is reflected by the box walls to between 5 and 15 5-inch photomultipliers connected together. Such veto counters with specially developed tubes by Photonis that sacrifice speed for improved photoelectron collection efficiency have been shown to give excellent particle separation signals, enabling a sharper veto than earlier gas counter designs.

Another use of the new aerogel is in the ring imaging Cherenkov (RICH) counters used in the HERMES experiment at DESY, Hamburg, Germany, which employs four thousand 19 mm diameter UV-glass Photonis photomultipliers.

8.4.2 Proton decay experiments

In ‘swimming-pool’ experiments (like the IMB detector, USA), in which the Cherenkov medium is a large volume of clean water, thousands of 5-inch ETL and later 8-inch hemispherical Hamamatsu photomultipliers were used to look for radiation due to proton decay. This decay has been predicted theoretically but as yet not observed. The IMB experiment was able to put the limit of proton life to at least 10^{32} years, thereby dismissing the first grand unification theory uniting all the known forces (the theory that set off the first race for the discovery of proton decay).

The KAMIOKANDE experiment in Japan used a thousand 20-inch hemispherical photomultipliers in an attempt to detect proton decay. This experiment (together with the IMB experiment) recorded the majority of the neutrinos detected on earth from the supernova 1987A*. The follow-up on the water-Cherenkov experiment, the SUPER KAMIOKANDE, used twelve thousand 20 inch Hamamatsu photomultipliers and had moved the limit of proton decay to more than 10^{33} years before an unfortunate accident caused a large number of the tubes to implode. The plan is to restore the experiment within the coming years. This, however, is not enough since one way to confirm modern physical theories would be to find proton decay existing (or not) in nature with a lifetime below 10^{35} years. Considerably larger experiments are therefore being proposed (HYPER KAMIOKANDE in Japan and UNO in the US) with more than 50 000 large photomultipliers each.

8.4.3 Solar neutrino experiments

The solar-neutrino flux has been found, by a massive thirty-year long deep-mine chlorine-to-argon solar neutrino-exchange-induced experiment, to be lower than

*Shared Nobel Prize in physics 2002

theoretically predicted* and several experiments have been designed to investigate the reason for this, which is supposed to be caused by the solar electron neutrino being changed into another ‘neutrino’ flavour, a phenomenon called ‘neutrino oscillation’.

The Solar Neutrino Observatory (SNO) in the Sudbury mine, Canada, makes use of around ten thousand 8-inch hemispherical Hamamatsu photomultipliers using heavy water (D₂O) as the Cherenkov medium. Recently published results indicate that the observed solar neutrino deficit indeed has its cause in neutrino oscillations.

The results are supposed to be confirmed by the boron-doped liquid-scintillator BOREXINO experiment in the Gran Sasso tunnel complex in Italy. This makes use of about fifteen hundred 8-inch ETL photomultipliers that start to collect data in 2003.

8.4.4 Neutrino oscillation experiments

To confirm that the neutrino flavour change (oscillations) is genuine, several large experiments have been built offering conflicting results. To confirm the debated results of a former liquid scintillator experiment in Los Alamos (LSND), a larger experiment, known as MiniBooNE at Fermilab, is just now starting to collect data. This makes use of about fifteen hundred 8-inch Hamamatsu photomultipliers. If the LSND results are confirmed, it will mean that there exists more than the three neutrino flavours of the standard model and will stimulate a need for an even larger experiment, i.e. BooNE, with more photomultipliers.

Two large experiments are already in construction, one in a mine in Minnesota (MINOS) as the target of a neutrino beam from Fermilab, and the other experiment in Gran Sasso, Italy, (OPERA), as the target of a neutrino beam from CERN, Geneva. Both will make use of emulsion detectors and plastic scintillators coupled via wavelength-shifting fibres to multichannel photomultipliers from Hamamatsu.

SUPER KAMIOKANDE, before its collapse, was already used, and will be used again, as the target of a neutrino beam from the Japanese KEK accelerator. It also has given convincing results in the study of atmospheric neutrinos, confirming that neutrino oscillations really occur in nature.

*Shared Nobel Prize in physics 2002

Since nuclear reactors are also a free source of neutrinos, several experiments have attempted to find neutrino oscillations by placing detectors at different distances from reactors, although with less convincing results so far. The hope is now that the KamLAND experiment, the old Kamioka detector filled with a liquid scintillator and using thirteen hundred 17-inch and seven hundred 20-inch Hamamatsu photomultipliers, will give convincing oscillation results. Because of its location, the experiment is sensitive to the reactor-generated neutrinos from 16 reactor sites (51 reactors) in Japan and 4 sites (18 reactors) in South Korea.

8.4.5 DUMAND* experiments

In the DUMAND Lake Baikal experiment, several hundred ‘smart’ 16-inch Russian photomultipliers are used on the bottom of the lake at a depth of 1400 m. This spectacular Cherenkov experiment will search for a theoretically predicted particle called the *magnetic monopole* (which has been proposed as the mechanism that triggers proton decay).

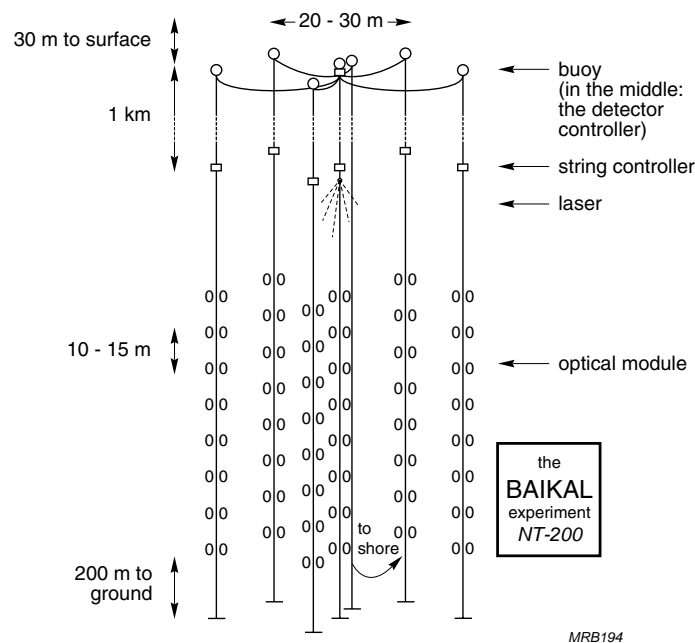


Fig.8.11 DUMAND Lake Baikal preliminary experiment (courtesy of INR, Moscow)

A similar arrangement on an even larger scale was planned for the DUMAND Hawaii experiment, where a cubic kilometre of ocean water was to be observed at 5 km depth to study possible galactic neutrino point sources. Although this DUMAND pioneer experiment was unfortunately cancelled, the extensive experience gained of

* Deep Underwater Muon And Neutrino Detector

The Photonis 15-inch ‘smart’ photomultiplier tube (see §1.5.6), which is capable of detecting low level multi-electron signals in a high single-photoelectron background environment, has been designed specifically for the Lake Baikal and Hawaii experiments. A Russian copy of the Photonis 15-inch ‘smart’ tube has also been developed for the Lake Baikal experiment. Although these ‘smart’ tubes are no longer in production, there is renewed interest in such tubes for extending the Baikal, NESTOR and NEMO experiments. Several new ideas are even now on the drawing boards of the photomultiplier suppliers to optimise the tubes for the new demands and for reducing costs.

8.4.6 Air-shower experiments

Cosmic-ray air showers, created when cosmic particles interact with the earth’s atmosphere at high altitude, are another source of Cherenkov radiation. In an extension to the HEGRA experiment on La Palma island, the Cherenkov radiation has been observed using a one square kilometre array of large hemispherical ETL photomultipliers combined with mirrors directed at the night sky (so called Aerobic detectors interest in which is also growing for an installation in India).

The EGRET experiment on board the Compton Gamma Ray Observatory satellite has demonstrated the existence of many γ -point sources with energies up to around 1 GeV. γ -ray telescopes are currently only able to detect γ -sources with energies above 1 TeV, and the present challenge for users of γ -ray telescopes is to extend their sensitivity to be able to detect γ -energies down to 1 GeV. There are therefore currently three new γ -ray telescope clusters in preparation:

- the HESS cluster of 16 telescopes on a high-plateau in Namibia, the first four using 960 29-mm-diameter low-afterpulse Photonis photomultipliers each
- the MAGIC planned cluster of three very large telescopes, the first one using 25 mm diameter hemispherical photomultipliers from ETL. This first telescope is now under construction at the HEGRA site at the La Palma island
- the VERITAS cluster of 7 telescopes. This is an extension of the Whipple site currently being prepared in the Arizona desert in which each telescope will use five hundred 29 mm diameter low-afterpulse UV-sensitive photomultipliers.

There exist spectacular cosmic phenomena seen by satellite and γ -ray telescopes, called gamma-ray bursts (GRB) – very-energetic, very-short-lived observations indicating an enormous cosmic energy “burst” of unknown origin. Further experiments are already being proposed to help investigators understand these GRBs.

Outside Salt Lake City, Utah, the Fly's Eye experiment has for the past few years been running the two so called HiRes eyes, providing a stereoscopic view from two mountain tops using 22 and 42 mirrors respectively, each focusing onto an array of two hundred and fifty six 39 mm hexagonal Photonis photomultiplier tubes. The experiment makes use of the nitrogen fluorescence UV lines stimulated by the secondary particles of the cosmic-ray air showers. Together with the older Japanese air-shower experiment, AGASA, the HiRes has recorded cosmic-ray events with an energy above 10^{20} eV, the highest cosmic ray energy ever recorded. This is in conflict with the GZK theory stating that events above about 10^{19} eV should not exist, the particle's energy supposedly being limited by interaction with the microwave cosmic ray background. To get more statistics to determine if such events are genuine, a third HiRes stereo-viewing eye on another mountain top with another 5 to 8000 tubes is planned.

This puzzle of the unexpected 'ankle' in the cosmic-ray spectrum has initiated the building of a very large air-shower detector at Malargüe, Argentina (see inside of the back cover), named AUGER after the first cosmic-ray air-shower experimentalist Pierre Auger who studied these showers using Geiger-Mueller tube coincidence signals in 1938. It consists of sixteen hundred 3 meter-diameter energy-autonomous water tanks, spread out over a very large area on the high-elevation pampas plateau. Each tank makes use of three Photonis 9-inch photomultipliers to detect the water-Cherenkov radiation originating from the air-showering particles. Complementing these are four fly's eye fluorescence detectors with more than 10 000 Photonis 38 mm hexagonal photomultipliers (as with the HiRes) to penetrate the atmosphere. If this "AUGER-South" detector is successful in detecting some high-energy ($>10^{20}$ eV) cosmic-ray events, the plan is to build a similar "AUGER-North" detector close to the HiRes in Utah, possibly making use of the HiRes as a fluorescent detector.

8.4.7 Towards a common goal

The DUMAND experiments are generally aimed at detecting very-high-energy neutrino cosmic point sources and the γ -ray experiments are looking for very-high-energy γ -ray bursts and γ -ray point sources with energies down to below 10 GeV. The air-shower experiments are looking for very-high-energy cosmic air-shower events. Although these are all different detection techniques, the common goal is to determine the nature of the gravitational energy-exchange processes believed to occur on a range of scales from binary-star systems and supernovae through to galactic nuclei, or to detect manifestations of cosmic forces and phenomena as yet unknown to mankind.

Finally, the apparent confirmation of neutrino oscillations implies that at least two of the traditional three neutrinos have mass. It also provides insight into the related challenge of understanding the possible charge-parity (CP) violation in the neutrino sector. This opens up a whole new aspect of neutrino physics – and the future need for new, extremely large experiments with very many photomultipliers. Owing to their large volume, these can also serve as proton-decay detectors.

8.4.8 A vital tool for physics

Cosmic-ray studies are not only opening up new and exciting areas in physics, they also provide a strongly growing market for photomultipliers whose combined traditional features of:

- large area coverage
- excellent time resolution
- low noise
- attractive price per square metre of detection

make them the only real choice for cosmic-ray research.

These combined features are, moreover, the principal reason why photomultipliers rapidly became the most widely used detector for early nuclear physics experiments, and it is also why they are likely to be the detectors of choice for the future generations of large astro-particle physics experiments in our new century. What is more, there is little doubt that all these new, very large experiments on the horizon will stimulate the development of ever larger tubes with lower noise (through ‘smartness’), higher quantum efficiency, pixelisation ‘smartness’ and, most important, low price per square metre of sensitive area.

The success of the photomultiplier over the past fifty years in meeting the challenges of the scientific community will doubtless continue into the future with completely new hybrid and ‘smart’ designs as yet only at the embryonic stage. No other detector known to mankind can match the photomultiplier’s sensitivity in detecting the fundamental particles that make up our physical world. No other detector is capable of penetrating so deeply into nature, and of providing us with such valuable insight into the nature of our universe.

Acknowledgements

We wish to thank the following persons for checking the accuracy of the details in this chapter and for all their enthusiastic and constructive comments:

John Learned, University of Hawaii, Honolulu, Hawaii, USA

John Matthews, University of Utah, Salt Lake City, Utah, USA

Peter Bosetti, RWTH Aachen, Germany and the Foundation Vijlen Institute for Physics, The Netherlands